THE JOURNAL OF PHYSICAL CHEMISTRY C

Article

pubs.acs.org/JPCC

Interpreting the First-Order Electronic Hyperpolarizability for a Series of Octupolar Push−Pull Triarylamine Molecules Containing Trifluoromethyl

Marcelo G. Vivas,*[,†,‡] Daniel L. Silva,[§] Ruben D. F. Rodriguez,[†] Sylvio Canuto,[∥] Jérémy Malinge,[⊥] Eléna Ishow,[#] Cleber R. Mendonca,[†] and Leonardo De Boni*[,†]

[†]Instituto de Física de São Carlos, Universidade de São Paulo, Caixa Postal 369, 13560-970 São Carlos, SP, Brazil

[‡]Instituto de Ciência de Tecnologia, Universidade Federal de Alfenas, Cidade Universitária—BR 267 Km 533, 37715-400 Poços de Caldas, MG, Brazil

[§]Departamento de Ciências da Natureza, Matemática e Educação, Universidade Federal de São Carlos, Rod. Anhanguera—Km 174,13600-970 Araras, SP, Brazil

[∥]Instituto de Física, Universidade de São Paulo, Caixa Postal 66318, 05314-970, São Paulo, SP, Brazil

[⊥]PPSM—UMR CNRS 8531, Ecole Normale Supérieure de Cachan, 61 avenue du Président Wilson, 94235 Cachan, France

[#]CEISAM—UMR CNRS 6230, Université de Nantes, 2 rue de la Houssinière, 44322 Nantes, France

ABSTRACT: In this present paper, we investigate the relationship between the dynamic first-order hyperpolarizability (DFH, or β_{HRS}) of a triarylamine core bearing two 3,3′-bis(trifluoromethyl)phenyl arms and the nature of a third group containing distinct electron-withdrawing strength (H < CN < CHO < NO_2 < Cyet < Vin). For that, we have combined hyper-Rayleigh scattering (HRS) experiments with picosecond pulse train at 1064 nm and quantum chemical calculations at the density functional theory (DFT) level. The β_{HRS} values exhibited pronounced enhancement from 56 × 10^{-30} cm^5/esu (EWG = CN) up to ∼400 × 10^{-30} cm^5/esu (EWG = Vin) due to the increase in the degree of donor−acceptor charge transfer concomitant with the intensification of the resonance enhancement effect observed when the scattered photon (2ω = 532 nm) approaches, in energy, the lowest energy band of chromophores. Furthermore, our experimental results suggest that the CF_3 group has a significant effect on the β_{HRS}, since we observed a considerable increase in this parameter (at least 30% higher) for CF_3EWG molecules as compared to their homologous tBu·EWG derivatives, recently investigated. Finally, the β_{HRS} results were compared with theoretical results provided by the coupled perturbed Hartree−Fock method implemented at the DFT level of theory and combined with a polarizable continuum model to take into account the solvent environment. The theoretical results allowed us to evaluate the effects of solvent-induced polarization and frequency dispersion on the first-order hyperpolarizability of the molecules and their molecular anisotropy (or dipolar/octupolar contributions).

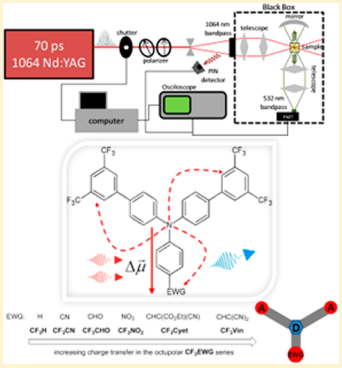

1. INTRODUCTION

The first-order hyperpolarizability (β) is a measure of how easily a dipole is induced in a molecule in the presence of an electric field ($\vec{E}$). Therefore, β is a quantitative measurement of the change in the charge distribution of an atom or molecule when it interacts with an electromagnetic wave.[1] At the macroscopic level, this effect is related to the second-order optical response, i.e., second-order susceptibility, $\chi^{(2)}$; therefore, it is, by nature, a nonlinear optical effect. To determine this important physical quantity in organic or inorganic materials, several techniques have been proposed.[1−7] Among them, the hyper-Rayleigh scattering (HRS) technique stands out because it is a simple technique that does not require complex mathematical analysis.[5−8] Basically, the HRS process involves the annihilation of two incident photons of frequency ω and the creation of a scattered photon at 2ω.[5,9] From the experimental point of view, a pulsed laser beam is focused at the middle point of a fused silica cuvette containing the material. The HRS signal emitted by the sample is collected perpendicular to the beam direction, avoiding a possible interference of the laser over the measured signal. Through the relationship between the intensities of the incident ($I(\omega)$) and scattering ($I(2\omega)$) beams, the dynamic first-order hyperpolarizability (DFH, or β) of a molecule can be measured. In general, to avoid considerable experimental errors, β is measured by using a reference material.

As a general rule, non-centrosymmetric organic molecules rich in π-electrons exhibit strong first-order hyperpolarizability; as a result, it has been used in several kinds of applications, includling efficient frequency doubling, high-resolution micros-

Received: March 11, 2015
Revised: May 1, 2015
Published: May 11, 2015

DOI: 10.1021/acs.jpcc.5b02386
J. Phys. Chem. C 2015, 119, 12589−12597

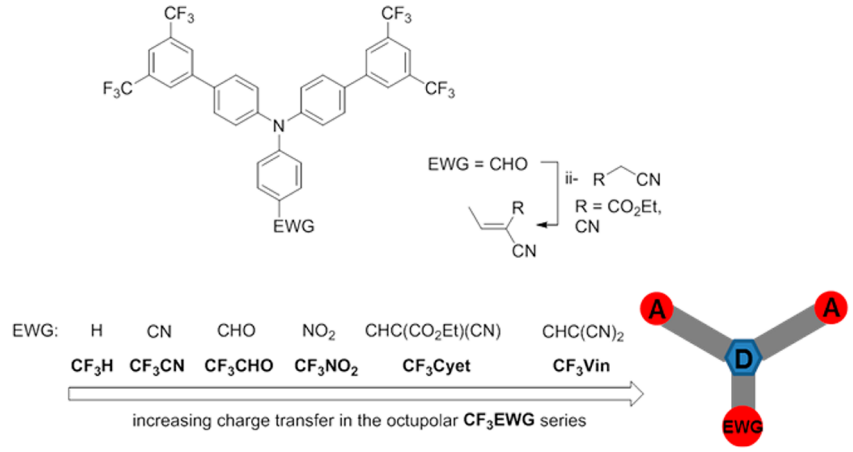

Figure 1. Molecular structure for the CF_3 triarylamine derivatives studied in this report.

copy, and fast electro-optic modulation.[10−16] On the other hand, first-order hyperpolarizability is absent in centrosymmetric molecules in an isotropic medium, because a perturbation caused by an electric field ($\vec{E}$) leads to a polarization in this kind of material ($\vec{P}^{(2)} = \chi^{(2)}:\vec{E}\vec{E}$) that does not alter its direction with respect to the reverse direction of the electric field ($-\vec{E}$).[17] However, some exceptions have been reported in the literature, since certain centrosymmetric molecules change drastically their molecular conformation due to distinct effects, such as solvent-induced effects, the application of an external electric field, and aggregate formation.[8,9,18,19]

The major aim in the design of molecules with remarkable first-order hyperpolarizability is to induce a large charge asymmetry in chromophores without greatly altering their molecular weight. For that, chemists and molecular engineers have focused attention on different molecular designs, such as dipolar (A-π-D), quadrupolar (A-π-D-π-A), and octupolar structures ((D-π-A)$_3$), where D and A refer to the electron-donating (donor) and electron-withdrawing (acceptor) groups, respectively, linked through a bridge of π-conjugated bonds. These structures contribute to improving the nonlinear hyperpolarizabilities of organic molecules due to the large charge separation induced and, consequently, produce chromophores with extraordinary optical and electronic features. Special attention has been given to designing push−pull octupolar structures since they have presented exceptional $\vec{\mu}$ and $\Delta\vec{\mu}$ values (between 10 and 30 D).[20−26] Thus, here we have studied the DFH magnitude for a series of push−pull triarylamine molecules as a function of the nature of different electron-withdrawing group (EWGs: H < CN < CHO < NO_2 < Cyet < Vin). These molecules present an octupolar structure consisting of a triarylamine core bearing two 3,3′-bis-(trifluoromethyl)phenyl arms and a third group with varying electron-withdrawing strength (see Figure 1). To determine the first-order hyperpolarizability, we performed HRS measurements with infrared (1064 nm) pulse trains containing approximately 20 pulses of 100 ps separated by 13 ns, delivered by a Q-switched and mode-locked Nd:YAG laser.[27] We also performed quantum chemical calculations combined with a polarizable continuum model (PCM) in order to determine the static ($\beta(0;0,0)$) and dynamic ($\beta(-2\omega;\omega,\omega)$) first-order hyperpolarizability of the molecules in toluene solvent and figure out the effect of the EWGs, the solvent-induced polarization, and the frequency dispersion on this nonlinear optical property.

Recently, some of us studied the two-photon absorption (2PA) properties of these molecules and found interesting results, in particular, large $\Delta\vec{\mu}$ values.[26] These results indicate that these molecules are potential candidates for applications involving second- and third-order optical processes.

2. EXPERIMENTAL SECTION

In order to obtain the first-order hyperpolarizability of the triarylamine derivatives dissolved in toluene, we used an extension of the conventional HRS technique involving picosecond pulse trains.[27] This extension, that has already been used in some published works,[28,29] allows to improve the HRS signal-to-noise ratio and speed up the acquisition process. High laser frequency rates indeed provide a better statistical ensemble, while mechanical control of the light intensity is no longer required. The technique takes advantage of a mode-locked and Q-switched pulse trains delivered by a solid-state Nd:YAG laser at 1064 nm. The pulse train has about 20 pulses with a 100 ps pulse width, separated by 13 ns. In our HRS setup, a mechanical shutter controlled by a computer is applied to block the laser beam during background determination and after the measurements, warranting that the sample is not exposed for a long time to the laser light. Additionally, two crossed polarizers are employed to limit a maximum laser intensity that pumps the sample. A fast (∼1 ns rise time) silicon detector (PIN) is used as a reference intensity channel. The laser beam is focused at the middle point of a 1 cm fused silica cuvette. The HRS signal emitted by the sample is collected perpendicularly to the pump beam direction, avoiding possible interferences of the laser with the measured signal. In order to improve the signal-to-noise ratio, our setup uses a spherical mirror to collect part of the signal that is scattered in the opposite direction of the photomultiplier tube (PMT, Hamamatsu H5783P).The back spherical mirror increases the HRS signal of about 100%. Between the sample and the PMT, a telescope is used to achieve a high solid angle. A narrow bandpass filter is used to allow only the 532 nm nonlinear scattering to be detected by the PMT. All system is enclosed in a black box. Measurements are averaged during 1 min using a laser repetition rate of about 300 Hz. After the sequence of HRS measurements, a linear absorption spectrum is recorded to observe possible photophysical degradations of the sample.

DOI: 10.1021/acs.jpcc.5b02386
J. Phys. Chem. C 2015, 119, 12589−12597

3. COMPUTATIONAL DETAILS

In this report, all the quantum chemical calculations were performed at the density functional theory (DFT) level.[30−32] To determine the effect of the toluene solvent on the equilibrium molecular geometry of the molecules, geometry optimization calculations were performed in the gas phase and also employing a PCM to take into account the solvent environment. The PCM using the integral equation formalism variant (IEF-PCM),[33,34] as implemented in Gaussian 09 package,[35] was employed for this purpose. The geometry optimization calculations were performed using the hybrid B3LYP[36,37] functional and the standard 6-311G(d,p) basis set.[38] It was not verified any important change between the molecular equilibrium geometries of each molecule obtained in the gas-phase or in solvent, calculated with the IEF-PCM model.

In the HRS experiment, the harmonic scattered light is given as the simple incoherent contribution of the scatterers. The intensity of the light scattered by a single molecule at the harmonic wavelength (2ω) is proportional to its orientational averaged first-order hyperpolarizability squared, $\langle\beta_{HRS}^2\rangle$ (the brackets indicate orientation averaging).[5] The relation between $\langle\beta_{HRS}^2\rangle$ and the components of the molecular first-order hyperpolarizability tensor (β_{ijk}) depends on the polarization state of the fundamental and harmonic beams, the spatial geometry of the experimental setup and the molecular symmetry.[39] In the classical HRS experiment, as conducted in this work, the 90° angle geometry is used.

The use of a description using spherical coordinates allows the β tensor (symmetric rank-3 tensor) to be decomposed, under the Kleinman's symmetry,[40] as the sum of a dipolar (J = 1) and an octupolar (J = 3) tensorial component. In this case, $\langle\beta_{HRS}\rangle$ can be written in function of the squared norms of the irreducible J spherical components as

$$\langle\beta_{HRS}\rangle = \sqrt{\frac{10}{45}|\beta_{J=1}|^2 + \frac{10}{105}|\beta_{J=3}|^2} \quad (1)$$

and the relationship between these two spherical components as determined experimentally and the molecular Cartesian components of β can also be found elsewhere.[41]

The nonlinear anisotropy parameter $\rho = |\beta_{J=3}|^2/|\beta_{J=1}|^2$ compares the relative contributions of the octupolar [$\Phi(\beta_{J=3}) = \rho/(1+\rho)$] and dipolar [$\Phi(\beta_{J=1}) = 1 - \Phi(\beta_{J=3})$] components to the first-order hyperpolarizability tensor β. Such parameter provides a quantitative classification of the molecular system in terms of its more or less pronounced octupolar/dipolar character.

In this study, the tensor components of the static and dynamic first-order hyperpolarizabilities have been analytically calculated by using the coupled perturbed Hartree−Fock method implemented at the DFT level of theory (coupled perturbed Kohn−Sham (CPKS) method). A series of works has already demonstrated that this approach is a good choice for the investigation of nonlinear optical properties of medium- and large-size systems because it combines both the quality of the results and the sparing of computational resources.[42−46]

The main aims of employing quantum chemical calculations in this work was to determine the equilibrium geometry of the derivatives, to address the effects of solvent-induced polarization and frequency dispersion on their electronic first-order hyperpolarizability and to determine their molecular anisotropy (or dipolar/octupolar contributions). In this report, we focus on the electronic contribution to the first-order hyperpolarizability and neglect the pure vibrational and zero-point vibrational average contributions. Although the pure vibrational contribution is negligible for SHG processes, the zero-point vibrational average contribution, on the other hand, is known to reach typically 10−15% of the electronic counterpart.[48−50] Nevertheless, the theoretical approach adopted herein is appropriate for a semiquantitative comparison between experimental data and theoretical values for β.

Through the description of the static/dynamic first-order hyperpolarizability using a two-level model (2LM),[51] one can realize the role of some molecular parameters to this nonlinear optical property. Adopting a 2LM, the static first-order hyperpolarizability can be expressed as

$$\beta_0(0;0;0) = \frac{3}{2}\frac{|\vec{\mu}_{01}|^2\cdot|\Delta\vec{\mu}_{01}|}{(\hbar\omega_{01})^2} \quad (2)$$

where $|\vec{\mu}_{01}|$ is the modulus of the transition dipole moment between ground (0) and first-excited (1) states, $|\Delta\vec{\mu}_{01}| = |\vec{\mu}_{11} - \vec{\mu}_{00}|$ is the modulus of the permanent dipole moment difference between ground and first-excited states, and $\hbar\omega_{01}$ is the energy of the electronic transition from ground to first-excited states.

In the context of the 2LM, extensively used to describe the nonlinear optical property of dipolar molecules, the relationship between static and dynamic first-order hyperpolarizabilities is given by a two-level β dispersion model which takes into account the resonance enhancement effect on the nonlinear property due to the optical frequency dispersion. The two-level β dispersion models differ by how they model the line-broadening of the optical transitions and the mechanisms behind it.[51−53] In the simplest model, called undamped 2LM, the static and dynamic first-order hyperpolarizabilities are related by the expression[51]

$$\beta(-2\omega;\omega,\omega) = D(\omega,\omega_{01})\beta_0 = \frac{{\omega_{01}}^4}{({\omega_{01}}^2 - 4\omega^2)({\omega_{01}}^2 - \omega^2)}\beta_0 \quad (3)$$

where $D(\omega,\omega_{01})$ is the frequency dispersion factor and ω is the angular frequency of the incident laser light. In this dispersion model, the frequency dispersion factor takes into account the resonance enhancement effect due to the optical frequency dispersion, but totally neglects the line broadening of the optical transition. Due to the total neglect of line broadening mechanisms, this factor diverges when the angular frequency of the incident laser light or its second harmonic (2ω) equals the angular frequency of the lowest-energy electronic transition of the molecule. Therefore, the undamped 2LM is expected to become inadequate as one enters the one- or two-photon resonance region. Nevertheless, thanks to its simplicity, this approach is the most popular one, used almost universally (although inappropriately) in experimental works to extrapolate dynamic first-order hyperpolarizabilities to the static limit, usually by estimating ω_{01} from linear absorption spectroscopy (maximum absorption).

It has been shown in recent years that the use of long-range corrected (LC) density functionals instead of the conventional exchange-correlation (XC) functionals provides theoretical predictions of β in better agreement with the experimental data. In fact, the conventional XC functionals have demonstrated serious drawbacks when applied to the calculation of nonlinear electric field responses.[54−56]

DOI: 10.1021/acs.jpcc.5b02386
J. Phys. Chem. C 2015, 119, 12589−12597

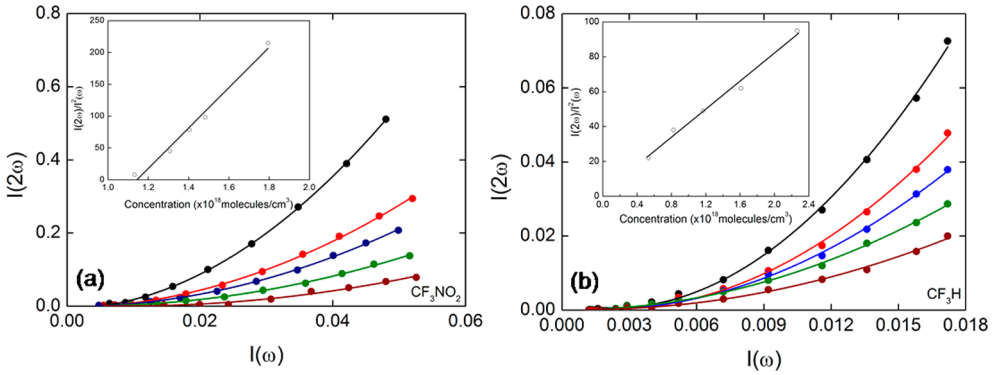

Figure 2. Experimental first-order hyperpolarizability scattering signal for five different concentrations of CF_3NO_2 (a) and CF_3H (b) triarylamine molecule dissolved in toluene. Solid lines show the second order polynomial dependence. The insets show the linear dependence between the hyperpolarizability signal and the concentrations. The concentration range was from 1×10^{17} to 2×10^{18} molecules/cm^3.

In a previous study conducted by some of us,[26] a preliminary assessment of the standard LC CAM-B3LYP functional fail to well reproduce the experimental UV−vis spectra of the molecules investigated herein. On the other hand, by following the successful strategy reported by Okuno,[57] we employed response functions calculations with the tuned CAM-B3LYP functional to fairly determine the lowest excitation energies of these molecules and to semiquantitatively reproduce their one- and two-photon absorption spectra. The default values of the CAM-B3LYP functional parameters are $\mu = 0.33$, $\alpha = 0.19$ and $\beta = 0.46$. In that previous study, based on the comparison between the energy of the one-photon lowest-energy transition determined by the PCM/response function calculation and the energy of the lowest-energy absorption band of the experimental UV−vis spectrum of the H molecule, the values of the CAM-B3LYP functional parameters were redefined for $\mu = 0.150$, $\alpha = 0.03$, and $\beta = 0.97$. Based on the results obtained in this previous study, we adopted the same reparametrization to employ the CAM-B3LYP functional in the present work.

The vertical electronic excitation energies and excited-state properties of the derivatives were computed employing the response function formalism at the DFT level of theory as implemented in the Dalton program.[58] The linear and quadratic response function calculations, both in gas phase and employing the PCM solvation method, were performed using the tuned CAM-B3LYP/6-311++G(d,p) approach. In the case of these calculations, the PCM as implemented in DALTON program was employed.[59] For consistency, for all molecules the van der Waals surfaces used in the response function calculations were defined by adopting the set of van der Waals radius and atomic centers determined at the geometry optimization stage using the Gaussian-09 package.

4. RESULTS AND DISCUSSION

The linear optical properties such as UV−vis spectra, fluorescence lifetime, and quantum yield for all CF_3EWG triarylamine derivatives studied here are described in details in ref 26. In that paper, we observed that all molecules present an intense absorption band in the UV range around 350−370 nm. A second absorption band appears at lower energy region in the visible range for CF_3NO_2, CF_3Cyet, and CF_3Vin derivatives.

Interestingly, compared to their homologous derivatives tBu·EWG,[60] the CF_3EWG series exhibit a bathochromic and hypsochromic shift of their UV and visible absorption bands, respectively. These observations suggest the electronic participation of the CF_3 groups on the charge transfer between the triphenylamino core and the EWG group.

Figure 2 depicts the typical experimental HRS signal (closed symbols) of one triarylamine compound dissolved in toluene for five different concentrations.

It is possible to perceive in insets of Figure 2 that the intensity of the first-order hyperpolarizability signal ($I(2\omega)/I^2(\omega)$) increases as the concentration increases (see inset), depicting a linear tendency. The same behavior was observed for the other compounds studied in this report. From the experimental data, the first-order hyperpolarizability can be obtained by taking the ratio between the angular coefficient (α) of the compound studied and reference material, which, in our case, was pNA dissolved in toluene ($\beta_{PNA} = (18 \pm 3) \times 10^{-30}$ cm^5/esu at 1064 nm, see ref 46).

The angular coefficient is acquired from the empirical relation between $I(2\omega)/I^2(\omega)$ (where $I(2\omega)$ is the intensity from the scattered beam at 2ω and $I(\omega)$ corresponds to the intensity of excitation beam) and sample concentration. In summary, first-order hyperpolarizability of our compounds can be calculated according to

$$\beta_{sample} = \beta_{reference}\sqrt{\frac{\alpha_{sample}}{\alpha_{reference}}} \quad (4)$$

In order to summarize the experimental first-order hyperpolarizability of all CF_3 triarylamine derivatives investigated in this study, we present in Table 1, together with the wavelength of maximum absorbance, the experimental values obtained using eq 4.

As can be seen in Table 1, in general, the DFH tends to increase (CN < H < CHO < NO_2 < Cyet < Vin) with the

Table 1. Experimental Values of the Wavelength of Maximum Absorbance (λ_{max}) in nm (and in eV in Parentheses) and the Dynamic First-Order Hyperpolarizability (β_{HRS}) in 10^{-30} cm^5/esu of All the Triarylamine Derivatives (CF_3EWG) Investigated

molecule	λ_{max} (E)	β_{HRS} at 1064 nm
CF_3H	361 (3.44)	102 ± 30
CF_3CN	347 (3.58)	56 ± 12
CF_3CHO	359 (3.46)	134 ± 20
CF_3NO_2	394 (3.15)	171 ± 30
CF_3Cyet	426 (2.91)	313 ± 55
CF_3Vin	439 (2.83)	770 ± 200

DOI: 10.1021/acs.jpcc.5b02386
J. Phys. Chem. C 2015, 119, 12589−12597

Table 2. Results of the CPKS Calculations Using the Tuned CAM-B3LYP/6-311++G(d,p) Approach for All Molecules Investigated[a]

		tuned CAMB3LYP-IOFs/6-311++G(d,p)										
		vacuum/vacuum					toluene/toluene					
molecule	ω	β_{HRS}	ρ	$\Phi(\beta_{J=1})$	$\Phi(\beta_{J=3})$	E_{0n} (nm)	β_{HRS}	ρ	$\Phi(\beta_{J=1})$	$\Phi(\beta_{J=3})$	E_{0n} (nm)	exptl (nm)
CF_3H	ω_0	19.8	2.50	0.285	0.715	363	28.8	2.42	0.293	0.707	371	361
	ω_1	42.9	2.34	0.299	0.701		64.6	2.28	0.305	0.695		
CF_3CN	ω_0	17.3	8.54	0.105	0.895	351	25.1	18.9	0.050	0.950	360	347
	ω_1	39.6	5.83	0.146	0.854		59.9	8.73	0.103	0.897		
CF_3CHO	ω_0	19.7	15.6	0.060	0.940	365	29.7	7.43	0.119	0.881	380	359
	ω_1	46.2	29.9	0.032	0.968		73.8	8.86	0.101	0.899		
CF_3NO_2	ω_0	22.4	3.74	0.211	0.789	385	38.7	2.39	0.295	0.705	411	394
	ω_1	58.3	2.80	0.263	0.737		126.2	2.02	0.331	0.669		
CF_3Cyet	ω_0	39.5	2.00	0.333	0.667	409	62.1	1.59	0.387	0.613	422	426
	ω_1	135.9	1.57	0.389	0.611		229.4	1.35	0.425	0.575		
CF_3Vin	ω_0	34.5	2.24	0.309	0.691	405	57.5	1.85	0.351	0.649	427	439
	ω_1	111.7	1.64	0.379	0.621		219.2	1.43	0.411	0.589		

[a]In addition to the static ($\omega = \omega_0$) and dynamic ($\omega = \omega_1$) first-order hyperpolarizabilities (β_{HRS}), given in 10^{-30} cm^5/esu, the table also shows the molecular anisotropy (ρ) according to the polarized HRS experiment, and the dipolar ($\Phi(\beta_{J=1})$) and octupolar ($\Phi(\beta_{J=3})$) contributions to the nonlinear optical property.

increase of EWG strength (H < CN < CHO < NO_2 < Cyet < Vin). However, it is noted that the DFH value obtained for the CF_3CN molecule is the lowest value found among all molecules, although the EWG strength for the CN group is higher than the H group. This observation is supported by the lower effective charge transfer (34%) and electronic coupling constant (240 meV) observed in CF_3CN molecule as compared with any another molecule studied in this report (see ref 26).

Another important outcome found in Table 1 is that β_{HRS} increases from 56 × 10^{-30} cm^5/esu in CF_3CN molecule to 770 × 10^{-30} cm^5/esu in CF_3Vin molecule. This great increase in DFH value is associated with the concomitant increase of donor−acceptor charge transfer and resonance enhancement caused by the Vin group on the triarylamine core. The resonance enhancement is due to the large red-shift (~750 meV) caused by the Vin EWG on the linear absorption spectrum as compared to the CN EWG. As a consequence, a considerable increase in the frequency dispersion factor ($D(\omega,\omega_{01})$) from 1.95 (CF_3CN) to 3.90 (CF_3Vin) is observed and contributes to increase β_{HRS}. It is worth to mention that this red-shift is caused by significant charge redistribution in the molecule due to the EWG = Vin. On the other hand, the donor−acceptor charge transfer among the arms of molecules can be quantified through the $|\vec{\mu}|$ and $|\Delta\vec{\mu}|$ parameters. Based on this statement, when we compare the $|\Delta\vec{\mu}_{01}|\cdot|\vec{\mu}_{01}|^2$ factor, to which β_{HRS} is proportional (eq 2), we observe an increase of ~4 times in β_{HRS} (in both cases, theoretical and experimental point of view) going from CF_3CN to CF_3Vin molecule. Therefore, according to our results, the main factor to the great increase of β_{HRS} for these molecules is the donor−acceptor charge transfer.

It is interesting to compare the DFH obtained for the CF_3EWG triarylamine derivatives with their homologous tBu·EWG, which has an electron-donating *tert*-butyl group in position 4 of the phenyl group instead of two-electron-acceptor trifluoromethyl groups.[46] The CF_3EWG series exhibit a considerable increase in β at 1064 nm (at least, 30% higher) as compared to their homologous tBu·EWG.[46] These observations suggest the effective participation of the CF_3 groups on the charge transfer between the triarylamine core and the EWG group. Indeed, CF_3EWG series exhibit a bathochromic and hypsochromic shift of their UV and visible absorption bands, respectively, corroborating the electronic participation of the CF_3 groups. It is important to mention, however, that our experimental error in determination of DFH is ~30% as shown in Table 1. To shed more light about the relationship between the effect of distinct EWG and the observed first-order hyperpolarizability activity, we have theoretically investigated the static $\beta_{HRS}(\omega=\omega_0)$ and dynamic $\beta_{HRS}(\omega=\omega_1)$ first-order hyperpolarizability of these CF_3 triarylamine molecules employing the CPKS method combined with a PCM. Table 2 gathers the results obtained by using the tuned CAM-B3LYP/6-311++G(d,p) approach for all molecules investigated in gas-phase and solvated. In addition the first-order hyperpolarizability values, the table also shows the molecular anisotropy (ρ) according to the polarized HRS experiment and the dipolar ($\Phi(\beta_{J=1})$) and octupolar ($\Phi(\beta_{J=3})$) contributions to the nonlinear optical property.

Concerning the solvent effects, the theoretical results indicate that the solvent-induced polarization enhances the static (intrinsic) first-order hyperpolarizability of all derivatives. The solvent-induced increase of the static first-order hyperpolarizability varies in the range of β = 5−73%. For the DFH the increase due to the interaction with the solvent environment is ascribed to both the solvent-induced polarization and the frequency dispersion effect. In this case, the solvent-induced increase varies in the range of β = 51−116%. A straight relation between the amplitude of the solvent-induced increase of both static and dynamic first-order hyperpolarizability (H = CN < CHO < Cyet < Vin < NO_2) and the strength of the EWGs (H < CN < CHO < NO_2 < Cyet < Vin) is not observed.

Regarding the dipolar and octupolar contributions to the magnitude of β, the theoretical results indicate that the CF_3 group produce an enhancement of the relative octupolar contribution in the DFH unlike their homologous tBu·EWG derivatives,[46] in which the relative dipolar and octupolar contributions are similar. However, the larger β_{HRS} values found here were for the CF_3Cyet and CF_3Vin molecules, which have the smallest relative octupolar contributions (<70%, see Table 2). This result can be explained because the Cyet and Vin radical are EWGs with strength higher than CF_3 group, and, therefore, as shown in ref 26, the donor−acceptor charge-transfer values to these groups (N → EWG) are higher than for

DOI: 10.1021/acs.jpcc.5b02386
J. Phys. Chem. C 2015, 119, 12589−12597

the others groups, increasing the dipolar contribution and, consequently, decreasing the octupolar/dipolar ratio for both molecules. This result does not mean that the absolute (and no the relative) octupolar contribution decreased for the CF_3Cyet and CF_3Vin molecules as compared to others, but that their dipolar contributions increase due to the great charge transfer on this arm. Therefore, as the nonlinear effect magnitude depends on two contributions (dipolar and octupolar), for these molecules the β tends to increase. Contrariwise, when the EWG has practically the same (or small) strength that the CF_3 group, the relative octupolar contribution tends to increase as observed for EWG = H, CN, COH, and NO_2 (see Table 2). This important outcome can explain, at least partially, the higher DFH values experimentally found for the CF_3EWG series as compared with their homologous tBu·EWG derivatives as previously reported.[46]

In Table 3, the value of the dynamic β as determined through the CPKS calculations and through the TD-DFT calculations in conjunction with the 2LM approach is shown for comparison purpose. The photophysical parameters used to describe the DFH value using the 2LM are depict in Table 4.

To better visualize these results, Figure 3 presents an illustrative comparison of the DFH values of all CF_3EWG derivatives determined from hyper-Rayleigh measurements (β_{exp}) with the 2LM approach and CPKS calculations.

Table 3. Dynamic First-Order Hyperpolarizability As Determined through the CPKS Calculation ($\beta_{HRS\text{-}CPKS}$) and the Two-Level Model Approach ($\beta_{HRS\text{-}2LM}$)

		$D_{CT}(\omega,\omega_{CT})$		$\beta_{HRS\text{-}2LM}(\omega=\omega_{CT})$	
molecule	$\beta_{HRS\text{-}CPKS}(\omega=\omega_1)$	theor	exptl	theor	exptl
CF_3H	64.6	2.20	2.09	47.8	43.6
CF_3CN	59.9	2.09	1.95	22.2	19.1
CF_3CHO	73.8	2.35	2.14	51.7	43.1
CF_3NO_2	126.2	3.04	3.09	125.0	128.2
CF_3Cyet	229.4	3.26	3.32	228.4	234.7
CF_3Vin	219.2	3.44	3.78	227.3	252.1

Table 4. Results of the TD-DFT Calculations Using the Tuned CAM-B3LYP/6-311++G(d,p) Approach for All CF_3 Triarylamine Derivatives[a]

molecule	n	E_{0n}	$\lvert\vec{\mu}_{0n}\rvert$	$\lvert\Delta\vec{\mu}_{0n}\rvert$
CF_3H	1	3.35	8.35	5.96
	2	3.64	1.25	0.48
CF_3CN	1	3.44	7.44	3.86
	2	3.50	6.68	7.47
CF_3CHO	1	3.26	7.72	6.66
	2	3.49	7.44	7.71
CF_3NO_2	1	2.98	7.70	10.53
	2	3.53	7.11	7.56
CF_3Cyet	1	2.93	10.49	9.30
	2	3.57	6.63	9.90
CF_3Vin	1	2.89	9.01	11.53
	2	3.53	6.96	8.84

[a] E_{0n} and μ_{0n} are the excitation energy and transition dipole moment of the two lowest-energy transitions of the derivatives. $\Delta\mu_n$ is the permanent dipole moment difference between the ground and n-excited states. The dipole moments are given in debye (D), while the excitation energies are given in electronvolts (eV).

Some points are clearly visualized in Figure 3. At first, it is observed a large disagreement between experimental and theoretical results for the CF_3Vin molecule in both panels a and b of Figure 3. This outcome can be explained because the CF_3Vin molecule has considerable 2PA at 1064 nm (~15 GM) that, consequently, will induce a fluorescence emission. This emission overlaps with the first-order hyperpolarizability signal (at 532 nm) and, therefore, as a result, we have an overestimated experimental value for the first-order hyperpolarizability of CF_3Vin as shown in Figure 3. For the others CF_3 compounds such phenomenon do not occur, since those do not present 2PA at 1064 nm and, therefore, a better agreement is observed between the experimental values and the results of the CPKS calculations. Based on the three-state model[61−63] and the photophysical parameters found in ref 26, we believed that the experimental DFH signal for the CF_3Vin molecule is overestimated by 80%.

Second, it is noted that the theoretical results provided by the CPKS ($\beta_{HRS\text{-}CPKS}(\omega=\omega_1)$) calculation and the 2LM approach ($\beta_{HRS\text{-}2LM}(\omega=\omega_1)$) are still smaller than the experimental data for all CF_3EWG molecules (see Figure 3), although the CPKS calculations are much closer to the experimental data. This occurs, most probably, because we did not observe, within the DFT framework, the influence of CF_3 group on the electronic structure of the octupolar molecules. Finally, comparing the CPKS results with the ones obtained using the 2LM approach, we clearly note that these results are in good agreement only for CF_3NO_2, CF_3Cyet, and CF_3Vin molecules. The poor agreement observed for the other molecules can be explained based on the high octupolar character (>70%, Table 2) of their DFH. As it is already well known,[61−63] in these cases the use of a three-state model is essential to properly model the DFH.

5. FINAL REMARKS

We have investigated the dynamic first-order hyperpolarizability for CF_3EWG molecules as a function of the nature of the electron-withdrawing groups by combining HRS measurements and quantum chemical calculations. Our results show that the DFH exhibits a great enhancement when the EWG = CN is substituted by EWG= Vin , more specifically, β_{HRS} increases from 56×10^{-30} cm^5/esu (EWG = CN) to ~400×10^{-30} cm^5/esu (EWG = Vin). We can mention at least two important features to explain this pronounced increase in β_{HRS}. The first is associated with the increase in the separation of charge induced by the Vin group on the triarylamine core ($|\Delta\vec{\mu}|$ increase from 9.0 to 13.5 D). The second is due to the increase in the frequency dispersion factor ($D(\omega,\omega_{01})$) from 1.95 (CF_3CN) to 3.90 (CF_3Vin) that takes place when the scattered photon (2ω = 532 nm) approaches the energy of the lowest energy band of the chromophores, increasing β_{HRS} enormously. It is worth mentioning that EWG = Vin causes a large red-shift (~750 meV) in the linear absorption spectrum as compared to EWG = CN. The quantum chemical calculations show that all molecules present predominant octupolar character. We attribute this outcome to the considerable charge asymmetry caused by the CF_3 group and distinct EWG on the triarylamine core, characterizing an octupolar structure. Although our experimental results suggested an effect of the CF_3 group in β_{HRS}, since we found higher DFH values for these molecules as compared to their tBu·EWG analogues,[46] the theoretical results (from the HOMO−LUMO analysis, see ref 26) do not support these data. In summary, our results shown that the CF_3 triarylamine derivatives have the potential to be applied in

DOI: 10.1021/acs.jpcc.5b02386
J. Phys. Chem. C 2015, 119, 12589−12597

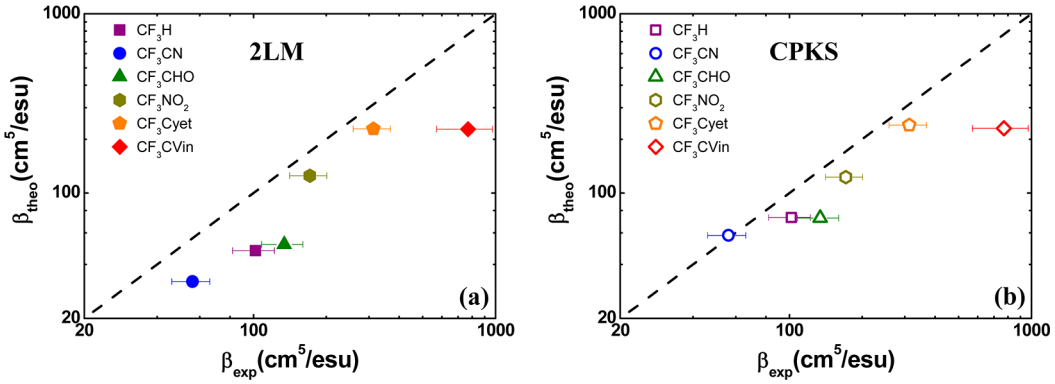

Figure 3. Theoretical values provided by (a) two-level model approach ($\beta_{HRS\text{-}2LM}(\omega{=}\omega_1)$, solid symbols) and (b) CPKS calculations ($\beta_{HRS\text{-}CPKS}(\omega{=}\omega_1)$, open symbols).

photonics devices that involve second- and third-order nonlinear optical effects.

AUTHOR INFORMATION

Corresponding Authors

*E-mail (M.G.V.): mavivas82@gmail.com.
*E-mail (L.D.): deboni@ifsc.usp.br.

Notes

The authors declare no competing financial interest.

ACKNOWLEDGMENTS

Financial support from Fundação de Amparo à Pesquisa do Estado de São Paulo (FAPESP, processo no. 2011/12399-0 and no. 2009/11810-8),Fundação de Amparo à Pesquisa do estado de Minas Gerais (FAPEMIG), Conselho Nacional de Desenvolvimento Científico e Tecnológico (CNPq), Coordenação de Aperfeiçoamento de Pessoal de Nível Superior (CAPES), and the Air Force Office of Scientific Research (FA9550-12-1-0028) is acknowledged.

REFERENCES

(1) Clays, K.; Persoons, A. Hyper-Rayleigh scattering in solution. *Phys. Rev. Lett.* **1991**, *66*, 2980−2983.
(2) Ostroverkhova, O.; Stickrath, A.; Singer, K. D. Electric field-induced second harmonic generation studies of chromophore orientational dynamics in photorefractive polymers. *J. Appl. Phys.* **2002**, *91*, 9481−9486.
(3) Carlotti, B.; Flamini, R.; Kikas, I.; Mazzucato, U.; Spalletti, A. Intramolecular charge transfer, solvatochromism and hyperpolarizability of compounds bearing ethenylene or ethynylene bridges. *Chem. Phys.* **2012**, *407*, 9−19.
(4) Sutherland, R. L. *Handbook of Nonlinear Optics*, 2nd ed.; CRC Press: New York, 2003.
(5) Clays, K.; Persoons, A. Hyper-Rayleigh scattering in solution. *Rev. Sci. Instrum.* **1992**, *63*, 3285−3289.
(6) Clays, K.; Persoons, A. Hyper-Rayleigh scattering in solution with tunable femtosecond continuous-wave laser source. *Rev. Sci. Instrum.* **1994**, *65*, 2190−2194.
(7) Franzen, P. L.; Misoguti, L.; Zilio, S. C. Hyper-Rayleigh scattering with picosecond pulse trains. *Appl. Opt.* **2008**, *47*, 1443−1446.
(8) Song, N. W.; Kang, T. I.; Jeoung, S. C.; Jeon, S. J.; Cho, B. R.; Kim, D. Improved method for measuring the first-order hyperpolarizability of organic NLO materials in solution by using the hyper-Rayleigh scattering technique. *Chem. Phys. Lett.* **1996**, *261*, 307−312.
(9) Yaliraki, S. N.; Silbey, R. J. Hyper-Rayleigh scattering of centrosymmetric molecules in solution. *J. Chem. Phys.* **1999**, *111*, 1561−1568.
(10) Ambekar, R.; Lau, T.-Y.; Walsh, M.; Bhargava, R.; Toussaint, K. C., Jr. Quantifying collagen structure in breast biopsies using second-harmonic generation imaging. *Biomed. Opt. Exp.* **2012**, *3*, 2021−2035.
(11) Benight, S. J.; Bale, D. H.; Olbricht, B. C.; Dalton, L. R. Organic electro-optics: Understanding material structure/function relationships and device fabrication issues. *J. Mater. Chem.* **2009**, *19*, 7466−7475.
(12) Dalton, L. R.; Sullivan, P. A.; Bale, D. H.; Bricht, B. C. Theory-inspired nano-engineering of photonic and electronic materials: Noncentro symmetric charge-transfer electro-optic materials. *Solid-State Electron.* **2007**, *51*, 1263−1277.
(13) DeWalt, E. L.; Begue, V. J.; Ronau, J. A.; Sullivan, S. Z.; Das, C.; Simpson, G. J. Polarization-resolved second-harmonic generation microscopy as a method to visualize protein-crystal domains. *Acta Crystallogr. Sect. D-Biol. Crystallogr.* **2013**, *69*, 74−81.
(14) Lau, T. Y.; Ambekar, R.; Toussaint, K. C., Jr. Quantification of collagen fiber organization using three-dimensional Fourier transform-second-harmonic generation imaging. *Opt. Exp.* **2012**, *20*, 21821−21832.
(15) Reeve, J. E.; Collins, H. A.; De Mey, K.; Kohl, M. M.; Thorley, K. J.; Paulsen, O.; Clays, K.; Anderson, H. L. Amphiphilic porphyrins for second harmonic generation imaging. *J. Am. Chem. Soc.* **2009**, *131*, 2758−2759.
(16) Tanabe, T.; Nishiguchi, K.; Kuramochi, E.; Notomi, M. Low power and fast electro-optic silicon modulator with lateral p-i-n embedded photonic crystal nanocavity. *Opt. Exp.* **2009**, *17*, 22505−22513.
(17) Hales, J. M.; Perry, J. W. *Introduction to organic electronic and Optoelectronic Materials and Devices*, 1st ed.; CRC Press: Orlando, 2008; Vol. *1*.
(18) Oudar, J. L.; Chemla, D. S. Hyperpolarizabilities of the nitroanilines and their relations to the excited state dipole moment. *J. Chem. Phys.* **1977**, *66*, 2667.
(19) Ray, P. C.; Das, P. K. Probing molecular self-assembly by hyper-Rayleigh scattering in solution. *Chem. Phys. Lett.* **1997**, *281*, 243−246.
(20) Campo, J.; Desmet, F.; Wenseleers, W.; Goovaerts, E. Highly sensitive setup for tunable wavelength hyper-Rayleigh scattering with parallel detection and calibration data for various solvents. *Opt. Exp.* **2009**, *17*, 4587−4604.
(21) Cardoso, C.; Abreu, P. E.; Nogueira, F. Structure dependence of hyperpolarizability in octopolar molecules. *J. Chem. Theory Comput.* **2009**, *5*, 850−858.
(22) Ronchi, M.; Pizzotti, M.; Biroli, A. O.; Righetto, S.; Ugo, R.; Mussini, P.; Cavazzini, M.; Lucenti, E.; Salsa, M.; Fantucci, P. Second-order nonlinear optical (NLO) properties of a multichromophoric system based on an ensemble of four organic NLO chromophores nanoorganized on a cyclotetrasiloxane architecture. *J. Phys. Chem. C* **2009**, *113*, 2745−2760.
(23) Van Cleuvenbergen, S.; Asselberghs, I.; Garcia-Frutos, E. M.; Gomez-Lor, B.; Clays, K.; Perez-Moreno, J. Dispersion overwhelms charge transfer in determining the magnitude of the first hyper-

DOI: 10.1021/acs.jpcc.5b02386
J. Phys. Chem. C 2015, 119, 12589−12597

polarizability in triindole octupoles. *J. Phys. Chem. C* **2012**, *116*, 12312−12321.
(24) Vivas, M. G.; Silva, D. L.; De Boni, L.; Bretonniere, Y.; Andraud, C.; Laibe-Darbour, F.; Mulatier, J. C.; Zalesny, R.; Bartkowiak, W.; Canuto, S.; et al. Experimental and theoretical study on the one- and two-Photon absorption properties of novel organic molecules based on phenylacetylene and azoaromatic moieties. *J. Phys. Chem. B* **2012**, *116*, 14677−14688.
(25) Vivas, M. G.; Silva, D. L.; De Boni, L.; Bretonniere, Y.; Andraud, C.; Laibe-Darbour, F.; Mulatier, J. C.; Zalesny, R.; Bartkowiak, W.; Canuto, S.; et al. Revealing the electronic and molecular structure of randomly oriented molecules by polarized two-photon spectroscopy. *J. Phys. Chem. Lett.* **2013**, *4*, 1753−1759.
(26) Vivas, M. G.; Silva, D. L.; Malinge, J.; Boujtita, M.; Zalesny, R.; Bartkowiak, W.; Agren, H.; Canuto, S.; De Boni, L.; Ishow, E.; et al. Molecular structure - optical property relationships for a series of non-centrosymmetric two-photon absorbing push-pull triarylamine molecules. *Sci. Rep.* **2014**, *4*, 4447.
(27) Franzen, P. L.; Zilio, S. C.; Machado, A. E. H.; Madurro, J. M.; Brito-Madurro, A. G.; Ueno, L. T.; Sampaio, R. N.; Barbosa Neto, N. M. Experimental and theoretical investigation of first hyperpolarizability in aminophenols. *J. Mol. Struct.* **2008**, *892*, 254−260.
(28) Dwivedi, Y.; De Boni, L.; Goncalves, P. J.; Mairink, L. M.; Menegatti, R.; Fonseca, T. L.; Zilio, S. C. Experimental and theoretical investigation of optical nonlinearities in (nitrovinyl)-1H-pyrazole derivative. *Spectrochim. Acta Part A-Mol. Biomol. Spectrosc.* **2013**, *105*, 483−487.
(29) Dwivedi, Y.; Tamashiro, G.; De Boni, L.; Zilio, S. C. Nonlinear optical characterizations of dibenzoylmethane in solution. *Opt. Commun.* **2013**, *293*, 119−124.
(30) Hohenberg, P.; Kohn, W. Inhomogeneous electron gas. *Phys. Rev. B* **1964**, *136*, B864−B871.
(31) Kohn, W.; Sham, L. J. Self-consistent equations including exchange and correlation effects. *Phys. Rev.* **1965**, *140*, A1133−A1138.
(32) Parr, R. G.; Yang, W. *Density-Functional Theory of Atoms and Molecules*; Oxford Univ. Press: Oxford, UK, 1989.
(33) Miertus, S.; Scrocco, E.; Tomasi, J. Electrostatic interaction of a solute with a continuum. A direct utilization of ab initio molecular potentials for the prevision of solvent effects. *Chem. Phys.* **1981**, *55*, 117−129.
(34) Tomasi, J.; Mennucci, B.; Cammi, R. Quantum mechanical continuum solvation models. *Chem. Rev.* **2005**, *105*, 2999−3093.
(35) Frisch, M. J.; et al. *Gaussian 09*; Gaussian, Inc.: Wallingford, CT, 2013.
(36) Becke, A. D. Density-functional thermochemistry. III. The role of exact exchange. *J. Chem. Phys.* **1993**, *98*, 5648−5652.
(37) Lee, C. T.; Yang, W. T.; Parr, R. G. Development of the colle-salvetti correlation-energy formula into a functional of the electron-density. *Phys. Rev. B* **1988**, *37*, 785−789.
(38) Frisch, M. J.; Pople, J. A.; Binkley, J. S. Self-consistent molecular-orbital methods 25. Supplementary functions for Gaussian basis sets. *J. Chem. Phys.* **1984**, *80*, 3265−3269.
(39) Günter, P. *Nonlinear Optical Effects and Materials*; Springer: Berlin/Heidelberg, 2000.
(40) Kleinman, D. A. Nonlinear dielectric polarization in optical media. *Phys. Rev.* **1962**, *126*, 1977−1979.
(41) Castet, F.; Bogdan, E.; Plaquet, A.; Ducasse, L.; Champagne, B.; Rodriguez, V. Reference molecules for nonlinear optics: A joint experimental and theoretical investigation. *J. Chem. Phys.* **2012**, *136*, 024506.
(42) Moreno Oliva, M.; Casado, J.; Lopez Navarrete, J. T.; Hennrich, G.; Delgado, M. C. R.; Orduna, J. Linear and nonlinear optical properties of pyridine-based octopolar chromophores designed for chemical sensing. Joint spectroscopic and theoretical study. *J. Phys. Chem. C* **2007**, *111*, 18778−18784.
(43) Orlando, R.; Lacivita, V.; Bast, R.; Ruud, K. Calculation of the first static hyperpolarizability tensor of three-dimensional periodic compounds with a local basis set: A comparison of LDA, PBE, PBE0, B3LYP, and HF results. *J. Chem. Phys.* **2010**, *132*, 244106.
(44) Lu, S.-I.; Chiu, C.-C.; Wang, Y.-F. Density functional theory calculations of dynamic first hyperpolarizabilities for organic molecules in organic solvent: Comparison to experiment. *J. Chem. Phys.* **2011**, *135*, 134104.
(45) Reish, M. E.; Kay, A. J.; Teshome, A.; Asselberghs, I.; Clays, K.; Gordon, K. C. Testing computational models of hyperpolarizability in a merocyanine dye using spectroscopic and DFT methods. *J. Phys. Chem. A* **2012**, *116*, 5453−5463.
(46) Silva, D. L.; Fonseca, R. D.; Vivas, M. G.; Ishow, E.; Canuto, S.; Mendonca, C. R.; De Boni, L. Experimental and theoretical investigation of the first-order hyperpolarizability of a class of triarylamine derivatives. *J. Chem. Phys.* **2014**, *142*, 064312.
(47) Bersohn, R.; Pao, Y. H.; Frisch, H. L. Double-quantum light scattering by molecules. *J. Chem. Phys.* **1966**, *45*, 3184.
(48) Dutra, A. S.; Castro, M. A.; Fonseca, T. L.; Fileti, E. E.; Canuto, S. Hyperpolarizabilities of the methanol molecule: A CCSD calculation including vibrational corrections. *J. Chem. Phys.* **2010**, *132*, 034307.
(49) Quinet, O.; Kirtman, B.; Champagne, B. Analytical time-dependent Hartree-Fock evaluation of the dynamic zero-point vibrationally averaged (ZPVA) first hyperpolarizability. *J. Chem. Phys.* **2003**, *118*, 505−513.
(50) Zoccante, A.; Seidler, P.; Christiansen, O. Computation of expectation values from vibrational coupled-cluster at the two-mode coupling level. *J. Chem. Phys.* **2011**, *134*, 154101.
(51) Oudar, J. L. Optical nonlinearities of conjugated molecules—tilbene derivatives and highly polar aromatic compounds. *J. Chem. Phys.* **1977**, *67*, 446−457.
(52) Campo, J.; Wenseleers, W.; Goovaerts, E.; Szablewski, M.; Cross, G. H. Accurate determination and modeling of the dispersion of the first hyperpolarizability of an efficient zwitterionic nonlinear optical chromophore by tunable wavelength hyper-Rayleigh scattering. *J. Phys. Chem. C* **2008**, *112*, 287−296.
(53) Orr, B. J.; Ward, J. F. Perturbation theory of non-linear optical polarization of an isolated system. *Mol. Phys.* **1971**, *20*, 513−526.
(54) Champagne, B.; Perpete, E. A.; Jacquemin, D.; van Gisbergen, S. J. A.; Baerends, E. J.; Soubra-Ghaoui, C.; Robins, K. A.; Kirtman, B. Assessment of conventional density functional schemes for computing the dipole moment and (hyper)polarizabilities of push-pull pi-conjugated systems. *J. Phys. Chem. A* **2000**, *104*, 4755−4763.
(55) Jacquemin, D.; Perpete, E. A.; Scuseria, G. E.; Ciofini, I.; Adamo, C. TD-DFT performance for the visible absorption spectra of organic dyes: Conventional versus long-range hybrids. *J. Chem. Theory Comput.* **2007**, *4*, 123−135.
(56) Kamiya, M.; Sekino, H.; Tsuneda, T.; Hirao, K. Nonlinear optical property calculations by the long-range-corrected coupled-perturbed Kohn−Sham method. *J. Chem. Phys.* **2005**, *122*, 234111.
(57) Okuno, K.; Shigeta, Y.; Kishi, R.; Miyasaka, H.; Nakano, M. Tuned CAM-B3LYP functional in the time-dependent density functional theory scheme for excitation energies and properties of diarylethene derivatives. *J. Photochem. Photobiol. A—Chemistry* **2012**, *235*, 29−34.
(58) *DALTON*, a molecular electronic structure program, Release 2.0, 2011; http://www.daltonprogram.org/.
(59) Frediani, L.; Rinkevicius, Z.; Agren, H. Two-photon absorption in solution by means of time-dependent density-functional theory and the polarizable continuum model. *J. Chem. Phys.* **2005**, *122*, 244104.
(60) Ishow, E.; Clavier, G.; Miomandre, F.; Rebarz, M.; Buntinx, G.; Poizat, O. Comprehensive investigation of the excited-state dynamics of push-pull triphenylamine dyes as models for photonic applications. *Phys. Chem. Chem. Phys.* **2013**, *15*, 13922−13939.
(61) Cho, M.; Kim, H. S.; Jeon, S. J. An elementary description of nonlinear optical properties of octupolar molecules: Four-state model for guanidinium-type molecules. *J. Chem. Phys.* **1998**, *108*, 7114−7120.
(62) Kanis, D. R.; Ratner, M. A.; Marks, T. J. Design and construction of molecular assemblies with large 2nd-order optical nonlinearities—quantum-chemical aspects. *Chem. Rev.* **1994**, *94*, 195−242.

DOI: 10.1021/acs.jpcc.5b02386
J. Phys. Chem. C 2015, 119, 12589−12597

(63) Suzuki, H.; Sukegawa, K. Evaluation of second-order hyperpolarizabilities for systems with low-energy double transitions by the three-level model. *Appl. Phys. Lett.* **1987**, *51*, 401−402.

DOI: 10.1021/acs.jpcc.5b02386
J. Phys. Chem. C 2015, 119, 12589−12597